

# SIMULATION OF HOT SPOTS GENERATION PROCESS ON SEPARATOR DISC IN MULTI-DISC CLUTCH

Cenbo Xiong<sup>a</sup>, Heyan Li<sup>a\*</sup>, Song He<sup>a</sup>, Biao Ma<sup>a</sup>, Qingdong Yan<sup>a</sup>, Hongcai Li<sup>a</sup>

Huiyu Xu<sup>b</sup>, Jianwen Chen<sup>b</sup>

<sup>a</sup> School of Mechanical Engineering, Beijing Institute of Technology, Beijing, 100081, China

<sup>b</sup> JiangLu Machinery & Electronics Group Co.,Ltd, Xiangtan City, Hunan province, 411100, China

\* Corresponding author. Tel.: +86-10-68918085; fax: +86-10-68918085. E-mail address:

[Lovheyan@gmail.com](mailto:Lovheyan@gmail.com) (Heyan Li).

## Abstract

In multi-disc clutches, the separator discs slide relatively to the friction discs during engagement, and usually display “hot spots” in a sinusoidal shape on both surfaces of a separator disc. Explanations based on “perturbation method” were widely used to describe the generation and development of hot spots in seals, brakes and clutches. In this study, a multi-disc clutch experiment was implemented to observe hot spots phenomenon, based on the results, a scenario of hot spots generation mechanism on thin disc is introduced and a 3D finite element non-uniform contact model of multi-disc clutch was developed to simulate the developing process of hot spots and illustrate the generation mechanism scenario.

Keywords: Multi-disc clutch; Hot spots; Generation mechanism

## 1. Introduction

Hot spots were commonly observed in brakes and clutches that may cause damage or even failure of these organs, many researches had been done to explain the causes and influences of hot spots on their serving performance. J. R. Barber proposed the concept of “Thermo-elastic Instability” (TEI) to describe the instability of railway braking systems which may fail due to the coupled thermal-elastic and wear effects between the braking block and the wheel<sup>1</sup>. TH. A. Dow and R. A. Burton introduced a perturbation method to calculate the temperature distribution and surface pressure at the interface between a thin blade and half-space<sup>2</sup>, this method related the heat transfer process with sliding speed and determined a “critical speed” for the frictional sliding system, the system would become unstable when surpassing the critical speed.

Anderson and Knapp classified hot spots obtained during automotive braking experiments and described

them as well as their possible causes in details<sup>3</sup>; Kasem used infrared camera to record the developing process of hot spots on a one-face brake during braking<sup>4</sup>; Burton observed the generation of hot spots in a transparent glass plate and metal cup friction system with temperature probes<sup>5</sup>.

In addition to experimental methods, considerable researches had been done theoretically to describe hot spots phenomenon. Zagrodzki used numerical methods to calculate the temperature distribution during the transient engagement of a multi-disc wet clutch and then analyzed it quasi-statically to obtain the stress distribution in the separator discs and friction discs<sup>6</sup>; He established a coupled thermal-elastic model which employed numerical methods to calculate the temperature field, thermal stress field and contact pressure distribution during severe engagement<sup>7</sup>. And also introduced a contact pressure perturbation to solve the coupled problem and studied the transient behavior of the engagement<sup>8,9,10</sup>.

Typical structure of multi-disc clutch is shown in Fig. 1a, the clutch embodies alternately assembled separator discs and friction discs as shown in Fig. 1b, and would engage or disengage under the pressure of control oil. Due to the structure and working limitation of multi-disc clutches, it's difficult to observe the generation process of hot spots or even measure the temperature distribution. The generation of hot spots is a coupled thermal-elastic problem, it's important to understand the interaction between temperature variation and out-of-plane deformation of the surfaces. Recently, Panier proposed a new progressive waviness distortion (PWD) theory based on plate theory (Kirchhoff assumption) and thermal-elastic theory to explain that the generation of macroscopic hot spots is related to the energy dissipated in the braking system<sup>11</sup>. In this paper, a similar scenario of hot spots generation process on thin discs named “hot

spots propagation mechanism” is proposed; a 3D finite element model of non-uniform contact is established to simulate the developing process of hot spots on the separator disc.

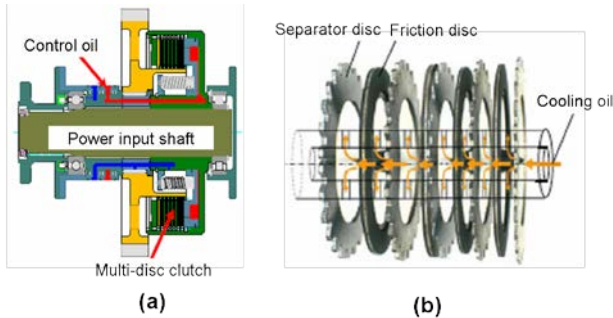


Fig. 1 Multi-disc clutch

## 2. Experiment

An experimental test bench was set up as shown in Fig. 2 to investigate the generation of hot spots on separator disc, the multi-disc clutch was assembled in a simplified transmission which is driven by electric motor and braked by hydraulic motor.

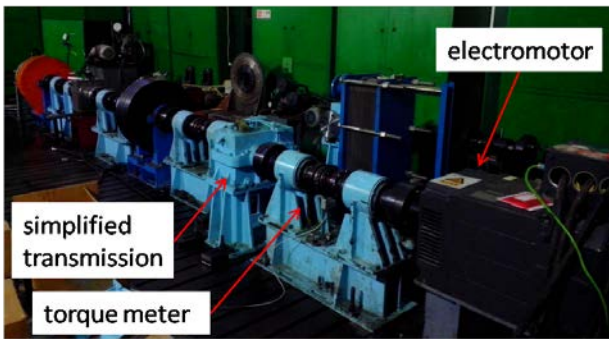


Fig. 2 Test bench of multi-disc clutch

The experiment was implemented mainly in the following steps: First, the control oil pressure was applied on the piston in the clutch and increased from 0 to 1MPa, the discs got into contact with each other statically; Second, hydraulic pressure was applied by the hydraulic motor to simulate the resistance of the vehicle before rotating of the drive shaft; Third, the rotating speed of electric motor started from 0 to 1000r/min, this process lasted for seconds. Hot spots could be found on some separator discs after the experiment, typical photos were taken as shown in Fig. 3.

Some obvious abrasion patches can be seen on the separator discs, they are hot spots produced during the engagement and distributed alternatively on both sides of the separator disc and located on the middle radius of the disc, which means that the high pressure contact area is on the middle radius.

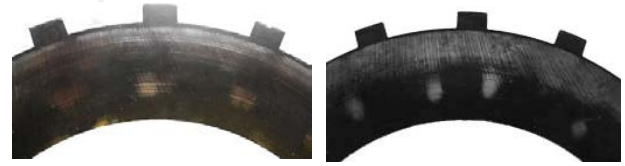


Fig. 3 Hot spots on separator discs

## 3. Generation mechanism hypothesis of hot spots on separator disc

The well known “Thermal-elastic Instability (TEI)” theory assumed a sinusoidal perturbation of temperature on the surface of a blade or a disc, with boundary conditions, critical speed for these organs could be figured out. While the generation and developing process of hot spots on thin discs may have alternative explanations. It is strongly influenced by the contact status of the two contacting surfaces as has been mentioned by a lot of researches in the past.

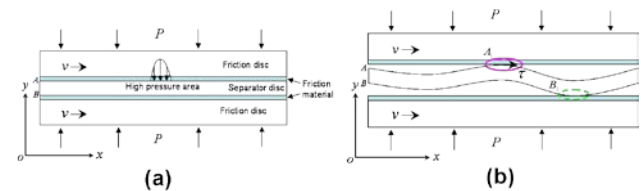


Fig. 4 Generation mechanism of hot spots on the separator disc

Based on the experimental phenomenon above, we assume that a local high pressure area exists on surface A of the separator disc which is caused by the non-uniform initial contact pressure distribution as shown in Fig. 4a. This area will be heated due to frictional heat flux and out-of-plane deflection is expected there. Under the effects of thermal banding, vertical pressure and shear traction on surface A, the disc would deform as shown in Fig. 4b and the first hot spot  $A_1$  emerges. In the down-flow direction of the relative velocity on surface B, the separator disc will bulge until getting into contact with the friction disc and a new hot spot  $B_1$  will be generated there in the same way as  $A_1$ .

This coupled thermal-elastic process can be illustrated detailedly in Fig. 5. An initial local high pressure emerges on surface A which inspires the coupled thermal-elastic process of hot spots. The hot spots developing process on one surface can be roughly divided into three steps: 1. Local heating; 2. Local bulging in the heated area; 3. Coupled thermal-elastic process to change the contact pressure.

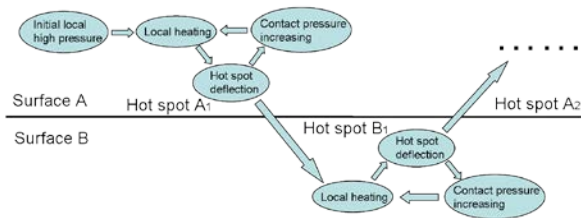


Fig. 5 Coupled thermal-elastic effect and propagation process of hot spots generation

These processes are repeated again and again and passed from one surface to the other on the disc until eventually a dissymmetric form of hot spots distribution is formed on the separator disc, which is similar to what mentioned by Lee and Barber<sup>5</sup>, this hot spots generation process can be introduced as “hot spots propagation mechanism”.

#### 4. Simulation of hot spots generation

A 3D coupled thermal-elastic model of clutch was established in finite element software ABAQUS in order to simulate the generation process of hot spots during a transient engagement.

##### 4.1 The model

Fig. 6a shows the 3D clutch model, part 1 and 3 are the friction discs, each one consists of a supporting plate (blue) and friction layer (brown), in order to simulate the higher pressure on the middle radius of the separator disc part 2, two ridges are designed in the radius interval of  $[0.095m, 0.11m]$  on both friction discs (Fig. 6c shows the enlarged local details). The distance between the steel disc and friction disc is enlarged for the convenience of observation.

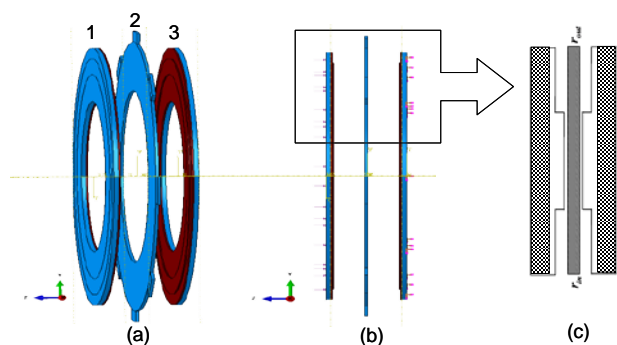


Fig. 6 The 3D non-uniform contact model of the clutch

In Fig. 6b, the back surface of friction disc 3 is fixed and a uniform axial load pressure is applied on the friction disc 1. Wear of the separator disc and friction disc is ignored in the model.

We assume the friction coefficient of the contact surfaces as a constant  $\mu = 0.1$ , axial pressure in the

model was applied before the rotation of the separator disc to avoid engagement impact at most. The relative load pressure and rotating amplitude curves are shown in Fig. 7 and the initial temperature of the whole model was designated to be  $20^{\circ}\text{C}$ . Since the engagement time was so short that the liquid cooling and heat radiation were negligible, thus the model was established as a dry friction system.

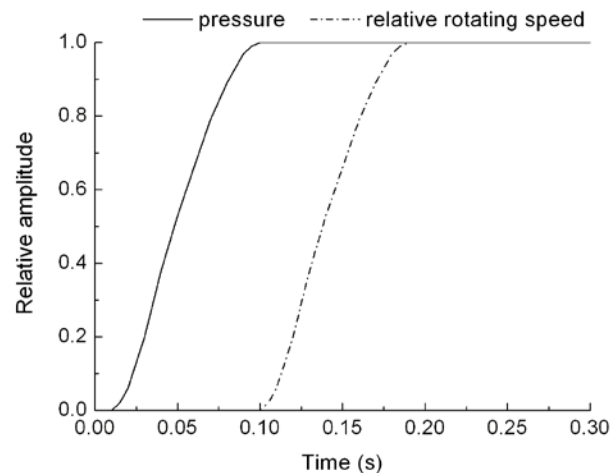


Fig. 7 Relative amplitude curves of pressure applied on the clutch and rotating speed

##### 4.2 Heat generation, separation and conduction

The material and geometric parameters of the separator disc and friction discs in the model are shown in Table 1.

Table 1 Material and geometric parameters of the model

Material Properties	Separator disc	Friction layer
Thermal Conductivity	42	8.5
Density(Kg/ m <sup>3</sup> )	7800	5500
Young's Modulus(Pa)	2.1E11	2.26E10
Poisson's Ratio	0.3	0.3
Expansion Coefficient(K <sup>-1</sup> )	5.27E-5	1.27E-5
Specific Heat(J/(kg · K))	452	600
Geometry Parameters	Separator disc	Contacting
Outer radius(m) (without teeth)	0.12	0.11
Inner radius(m)	0.08	0.095
Thickness(m)	0.002	

On contact surfaces, the heat flux  $q_f$  generated by frictional sliding can be expressed as:

$$q_f = \eta \tau v \quad (1)$$

Where  $\eta$  is the conversion factor of friction work to heat,  $\tau = p\mu$  is the frictional stress between the contacting surfaces which has relationship with the axial pressure  $p$ , friction coefficient  $\mu$  and also with the temperatures on both interacting faces,  $v = r\omega$  is the relative sliding speed between the contacting surfaces.

The heat is separated and conducted to both of the contacting surfaces immediately when it's generated. According to Tien-Chen Jen's research<sup>12</sup>, following the continuous conditions of temperature and heat flux on the interface between different materials, the ratio of the separated heat between the surfaces can be expressed as:

$$\frac{q_1}{q_2} = \frac{\lambda_1}{\lambda_2} \sqrt{\frac{\alpha_2}{\alpha_1}} \quad (2)$$

Where  $q_1$  and  $q_2$  denotes the heat flux conducted into the friction disc and separator disc separately as shown in Fig. 8. From the expression, we can see that the heat separation depends on the material properties of the contacting surfaces. For the given materials, the ratio is  $\frac{q_1}{q_2} = \frac{3}{7}$  which means that 70% heat is conducted into the separator disc.

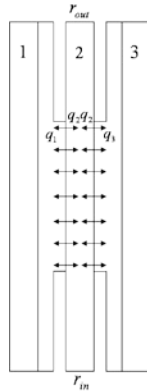


Fig. 8 Heat generation and conduction between the discs

The temperature field in the separator disc can be calculated by the transient heat conduction equation, since there is no internal heat source, the equation can be expressed in cylindrical coordinates as:

$$\rho c \frac{\partial T}{\partial t} = \frac{1}{r} \frac{\partial}{\partial r} \left( \lambda_r r \frac{\partial T}{\partial r} \right) + \frac{1}{r^2} \frac{\partial}{\partial \theta} \left( \lambda_\theta \frac{\partial T}{\partial \theta} \right) + \frac{\partial}{\partial z} \left( \lambda_z \frac{\partial T}{\partial z} \right) \quad (3)$$

There is only heat flux boundary condition on the contacting surface  $S_q$ , that is

$$\lambda_r \frac{\partial T}{\partial r} n_r + \lambda_\theta \frac{\partial T}{\partial \theta} n_\theta + \lambda_z \frac{\partial T}{\partial z} n_z = q \quad (4)$$

For homogenous materials,  $\lambda_r = \lambda_\theta = \lambda_z = \lambda$  is the thermal conductivity, the governing equation and heat flux boundary condition can be simplified as:

$$\frac{\partial T}{\partial t} = a \left[ \frac{1}{r} \frac{\partial}{\partial r} \left( r \frac{\partial T}{\partial r} \right) + \frac{1}{r^2} \frac{\partial^2 T}{\partial \theta^2} + \frac{\partial^2 T}{\partial z^2} \right] \quad (5)$$

$$\lambda \left( \frac{\partial T}{\partial r} n_r + \frac{\partial T}{\partial \theta} n_\theta + \frac{\partial T}{\partial z} n_z \right) \Big|_{S_q} = q \quad (6)$$

where  $a = \frac{\lambda}{\rho c}$  is thermal diffusivity of the separator disc

material, neglecting the convective and radiation heat dissipation, with weighted residual method, the equivalent integration formation of this problem is:

$$\int_V w \left[ \rho c \frac{\partial T}{\partial t} - \frac{\lambda}{r} \frac{\partial}{\partial r} \left( r \frac{\partial T}{\partial r} \right) - \frac{\lambda}{r^2} \frac{\partial^2 T}{\partial \theta^2} - \lambda \frac{\partial^2 T}{\partial z^2} \right] dV + \int_{S_q} w_1 \left[ \lambda \left( \frac{\partial T}{\partial r} n_r + \frac{\partial T}{\partial \theta} n_\theta + \frac{\partial T}{\partial z} n_z \right) - q \right] dS = 0 \quad (7)$$

For the arbitrariness of weight function in Galerkin method, we choose

$$w = w_1 = \delta T \quad (8)$$

Using Guassian theorem, the weak form of equation 7 can be expressed as:

$$\int_V \rho c \delta T \frac{\partial T}{\partial t} dV - \int_{S_q} \delta T q dS + \int_V \lambda \left[ r \frac{\partial T}{\partial r} \frac{\partial}{\partial r} \left( \frac{\delta T}{r} \right) + \frac{\partial T}{\partial \theta} \frac{\partial}{\partial \theta} \left( \frac{\delta T}{r^2} \right) + \frac{\partial T}{\partial z} \frac{\partial \delta T}{\partial z} \right] dV = 0 \quad (9)$$

The temperature  $T$  in this model can be approximated by:

$$T = \tilde{T} = \sum_{i=1}^{n_e} N_i(r, \theta, z) T_i(t) \quad (10)$$

Where  $N_i(r, \theta, z)$  are shape functions and  $T_i(t)$  are the nodal temperature values, substituting equation 10 into equation 9 and choosing the shape function as the weight function results in the discrete finite element form:

$$\int_V \rho c N_i N_j \dot{T}_j dV - \int_{S_q} N_i q dS + \int_V \lambda \left[ r \frac{\partial N_j}{\partial r} \frac{\partial}{\partial r} \left( \frac{N_i}{r} \right) + \frac{1}{r^2} \frac{\partial N_j}{\partial \theta} \frac{\partial N_i}{\partial \theta} + \frac{\partial N_j}{\partial z} \frac{\partial N_i}{\partial z} \right] T_j dV = 0 \quad (11)$$

Simplify this equation to be matrix form:

$$\dot{C}T + KT = P \quad (12)$$

These are a set of ordinary differential equations and all the matrix coefficients are lamped by elements:

$C_{ij} = \sum_e C_{ij}^e$ , where  $C_{ij}^e = \int_{V^e} \rho c N_i N_j dV$  is the element

specific capacity matrix.

$K_{ij} = \sum_e K_{ij}^e$ , Where

$$K_{ij}^e = \int_{V^e} \lambda \left[ r \frac{\partial N_j}{\partial r} \frac{\partial}{\partial r} \left( \frac{N_j}{r} \right) + \frac{1}{r^2} \frac{\partial N_j}{\partial \theta} \frac{\partial N_i}{\partial \theta} + \frac{\partial N_j}{\partial z} \frac{\partial N_i}{\partial z} \right] dV$$

is the element heat conduction matrix.

$$P_i = \sum_e P_{q_i}^e, \text{ where } P_{q_i}^e = \int_{S_q} N_i q dS \text{ is the heat flux load}$$

boundary condition vector.

This equation can be solved by direct integration method and the backward difference algorithm is used since it is unconditionally stable.

### 4.3 Thermal-elastic problem

The thermal deformation and stresses in the model can be calculated since the temperature field had been figured out. Using the variational principle, the finite element equilibrium equation for the discs can be expressed in matrix form as

$$KU = P + P_T \quad (13)$$

Where

$$K = \sum_{e=1}^{n_e} k^e, \quad k^e = \int_{V^e} B^T D B dV \text{ is the element stiffness}$$

matrix.  $P = \sum_{e=1}^{n_e} \int_S N^T F dS$  is the load vector on the

surfaces,  $N$  is the shape function and  $F$  is the force vector applied on the surfaces.  $P_T = \sum_{e=1}^{n_e} \int_V B^T D \varepsilon_0 dV$  is

the equivalent load caused by temperature variation in the domain where  $B$  is the strain matrix,  $D$  is the elastic matrix and  $\varepsilon_0 = \alpha \Delta T$  denotes the strain result from the temperature variation.

The displacement  $U$  of the discs could be calculated from equation 13, the explicit central-difference integration rule is used to obtain the mechanical response with a lumped mass matrix, the heat transfer and mechanical solutions are obtained simultaneously by an explicit coupling, because both the forward-difference and central-difference integrations are explicit, no iterations or tangent stiffness matrices are required for explicit integration, it can be less expensive computationally and the contact problem can be simplified<sup>13</sup>.

### 5 Simulation and results

In the simulation, we applied uniform pressure on the friction disc that induced 1MPa nominal pressure on the contact interface, the friction discs didn't rotate and the separator disc rotated from 0 to 1000 rpm in 0.3s following the rotating speed amplitude curve in Fig. 7. The whole simulation period was 0.32s with 0.02s for applying the axial pressure and 0.3s for rotating.

There are 30000 elements in the model, due to the tiny deformation in the hot spots area, it is reasonable to

adopt the linear coupled "solid temperature-displacement" element C3D8RT which is an 8-node trilinear displacement and temperature element, reduced integration with hourglass control. This type of element doesn't include geometrical nonlinear, so we used 8 elements along the thickness of the separator disc to increase the bending stiffness.

There were 750710 time increments in the whole simulation process and the stable time increment was 4.01237e-7s. With the simulation results, we can see the generation process of hot spots on the surfaces of the discs.

### 5.1 The generation of hot spots

The surfaces of the discs were flat at the very beginning of the simulation in this ABAQUS model, but when the axial pressure was applied on the friction disc and rotating torque was applied on the separator disc respectively, the surfaces of the separator disc had some tiny initial non-uniform axial deflection, this could be considered as the initial perturbation on the surface just as roughness on practical discs. Because of the coupled thermal-elastic effect, the initial axial displacement fluctuation was enlarged until the first local hot spot formed. Extracting the axial displacement and temperature data from all 560 points evenly along a circle path through all the hot spots on the upside and downside surfaces of the separator disc, we can reveal the generation and developing process of hot spots.

Fig. 9 shows the axial displacement and temperature variations along the circumference of the separator disc at three moments. In Fig. 9a, an initial bump formed between the area from node number 460 to 500 because of the non-uniform heat input on the upside and downside surfaces at time  $t = 0.064s$  and the temperature there is accordingly much higher than other places which means the first hot spot had formed there. The temperature distribution there is not symmetric about the middle plane, the temperature on the downside surface is lagged than the upside surface. In the area between node 503 to 507, the temperature on the downside surface is much higher than the upside surface so that thermal stress and moment emerged there and forced the plate to bend towards the upside direction.

When comes to the moment  $t = 0.065s$ , because the upside surface contacts with the frictional disc and be heated, the displacement and temperature increase sharply until the second hot spot emerges there as shown in Fig. 9b, and the temperature there raised sharply from the initial temperature 20°C to 300°C on average.

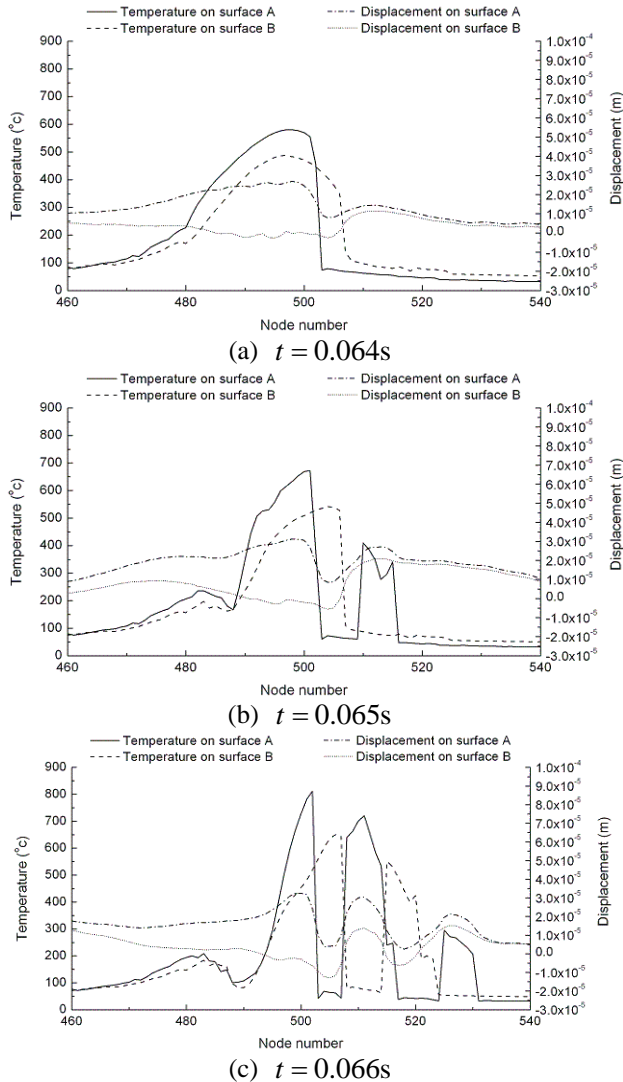


Fig. 9 The axial displacement and temperature variation along the circle on the upside and downside surfaces of the separator disc

When comes to the moment  $t = 0.066s$  as shown in Fig. 9c, there are already two hot spots on the upside and downside surfaces, following the same process, a third hot spot is forming on the upside surface. Hence, this process can be conclude as: because of the non-uniform heat input, once an initial local hot spot been generated on one surface, under the thermal stress and axial pressure, the nearby area on the other surface in the downstream direction of the velocity will get into contact with the friction surface and another hot spot will develop on this surface, the same process will repeat again and again between the two surfaces until the hot spots have been distributed along the whole circumference, finally the hot spots distribute alternatively on the two surfaces of the separator disc in a sinusoidal shape. All the hot spots emerged in a short

time that depends on the energy flows into the separator disc. The deformed separator disc with hot spots is shown in Fig. 10 where the axial displacement is enlarged 30 times for the convenience of observation.

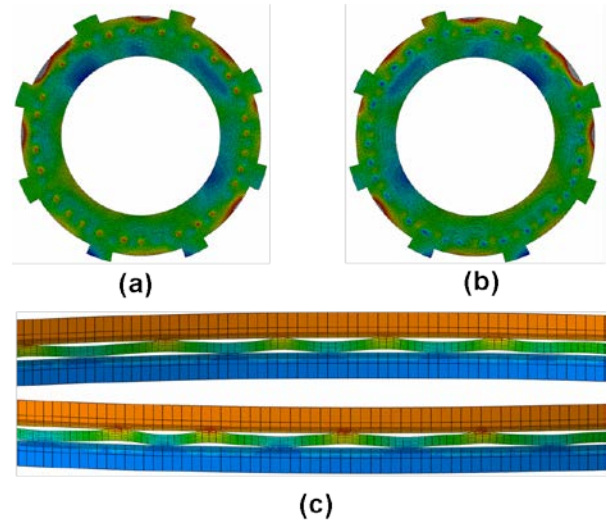


Fig. 10 Hot spots and axial deformation of the separator disc

Fig. 10a and Fig. 10b shows the hot spots on the upside and downside surfaces of the separator disc respectively, Fig. 10c shows the sinusoidal axial deformation of the separator disc, similar distributions of hot spots were also observed by Burton<sup>11</sup>. Since the number of hot spots and their distribution on the separator disc is strongly influenced by the working conditions, material properties and dynamic processes of the clutch, they may not exactly evenly distributed along the circle, hence we can define average wavelength

$$\lambda = \frac{L}{n}$$

$L = 0.644$  is the perimeter of the circle, the more hot spots on the circle the short the wavelength would be. Here in this work, several simulations were done with different contact pressure, rotating speed, Young's modulus and thermal expansion coefficient to investigate their influence on the hot spots wavelength.

## 5.2 The effect of contact pressure

The number of hot spots is directly related to the engagement pressure, relative rotating speed and consequent relationship with the heat flux generated by friction.

The engagement pressure, applied by the hydraulic piston, will not only influence the heat generation of the steel disc but will also suppress the axial displacement of the hot spots. Fig. 11 shows the relationship between the hot spots number and the contact pressure, the Young's modulus of the steel disc was kept at a constant  $200GPa$ ,

the thermal expansion coefficient was  $5 \times 10^{-5} \text{ K}^{-1}$  and the rotating speed was 1000r/min .

From the trend line we can conclude that as  $p$  increases from 0.2MPa to 2.6MPa , the hot spots number decreases linearly. There are 32 hot spots corresponding to 0.2MPa and 24 hot spots corresponding to 2.6MPa . When the contact pressure is small, the deformation remains in a "hot band" mode, which eventually becomes separated hot spots, this evolution occurs because of the small heat production and insufficient expansion. Since the tangential frictional force is insufficient to cause the steel disc to buckle and generate subsequent hot spots, it is only when the heat had been accumulated to a certain level that an initial hot spot can be generated.

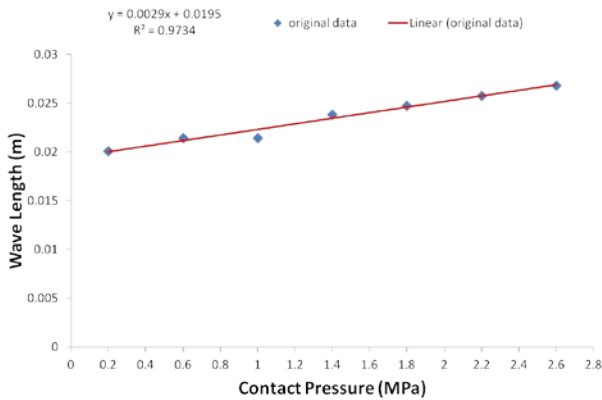


Fig. 11 Influence of contact pressure on the hot spots wavelength

### 5.3 The effect of rotating speed

According to the experimental results of Panier<sup>17</sup>, only when the load had reached a certain level can the hot spots be produced even if the relative rotating speed had achieved a certain value, this result reveals that the rotating speed is not a significant factor of hot spots. The relative sliding speed of the separator disc directly affects the heat flux, and thereby affects the initial hot spots wavelength. Since the final distribution of hot spots in the circumferential direction is generated by propagation, all hot spots wavelengths would be affected by the rotating speed.

Fig. 12 shows that when the separator disc rotates under the pressure 0.2MPa , 0.6MPa and 1.0MPa , the hot spots wavelength linearly increases during the rotating speed between 200r/min to 4000r/min .

The lines show that rotating speed affects the hot spots wavelength in a wide range. Regular hot spots distributions could be obtained even at a slow rotating speed such as 200r/min .

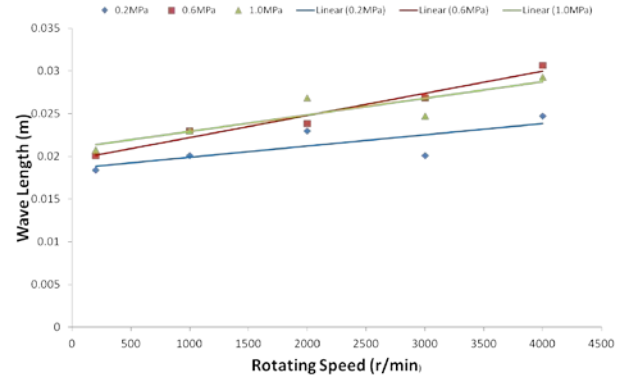


Fig. 12 Influence of rotating speed on the hot spots wavelength

### 5.4 The effect of Young's modulus

Commonly used material for practical clutches and experimental studies has fixed physical properties, the present study fixes the friction disc material parameters but changes the separator disc material parameters. Fig. 13 shows the relationship between the steel's Young's modulus  $E$  and hot spots wavelength  $\lambda$  , the wavelength variation under the axial pressure of 0.2MPa , 0.6MPa and 1.0MPa was obtained.

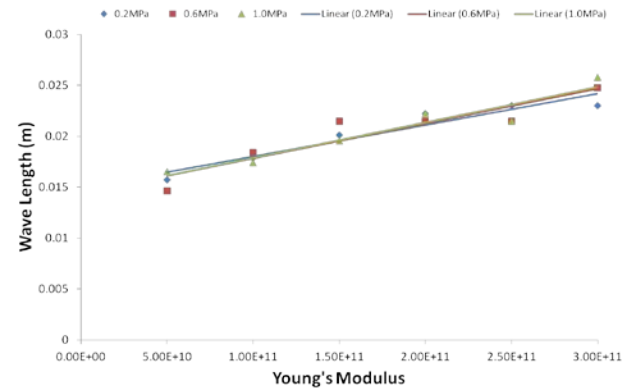


Fig. 13 Influence of steel's Young's modulus on the hot spots wavelength

From Fig. 13 we can see that the hot spots wavelength increases when the steel's Young's modulus increases, which means that the deformation of the separator disc becomes increasingly difficult. When  $E$  reaches  $3 \times 10^{12}$  GPa, The number of hot spots will drop dramatically to only 13 and the corresponding wavelength reaches 0.05m, when the Young's modulus decreases, the number of hot spots will increase until there is no individual hot spot.

### 5.5 The effect of thermal expansion coefficient

Since the thermal expansion coefficient  $\alpha$  of commonly used steel is about  $5 \times 10^{-5} \text{ GPa}$ , studies with wider range

of  $\alpha$  as shown in Fig. 14 indicate that when  $\alpha$  becomes larger, the wavelength of hot spots becomes longer, and the minimum number of hot spots is only 1 which is similar to Burton's conclusions<sup>11</sup>; when  $\alpha$  becomes smaller, the wavelength of hot spots becomes shorter until a hot band formed.

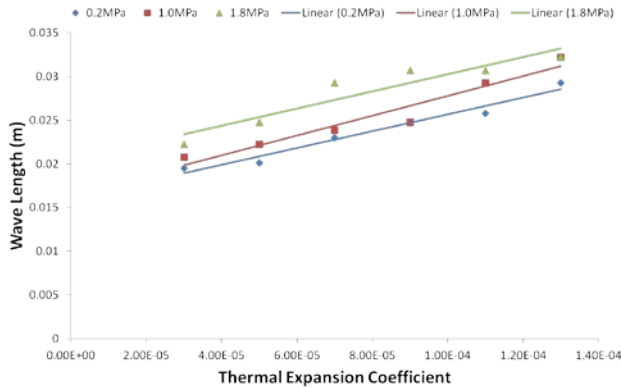


Fig. 14 Influence of thermal expansion coefficient on the hot spots wavelength

## 6. Conclusions and Discussions

By using finite element method, the developing process of hot spots on the separator disc during the engagement of a practical multi-disc clutch was studied, and a propagation mechanism scenario of hot spots was introduced. This mechanism is divided into three phases: First, initial local heating causes local hot expansion and the first hot spot is formed; Second, due to thermal stress, another hot spot is produced alternatively on the other side of the separator disc; Third, more hot spots form on the disc following the same way of propagation until a sinusoidal shape deformation with hot spots over the entire circumference is achieved.

A serial of simulations show that when the load pressure, rotating speed, Young's modulus and thermal expansion coefficient of the separator disc increase, the hot spots wavelength will increase almost linearly.

These results were calculated by reliable FE code, they can illustrate the hot spots generation mechanism scenario correctly and forecast the trend of hot spots wavelength's dependency on some working conditions, and also provide insights for clutch design. However, due to the complicity of 3D model, load pattern, dynamic impact and ignorance of wear, the axial displacement and the wavelength of hot spots are not so accurate, in the future, more accurate model need to be set up to obtain more accurate results of this problem.

## 7. Acknowledgements

The authors would like to acknowledge the financial support by National Natural Science Foundation of China (Grant No.51175042 and No.51005021).

## 8. References

- <sup>1</sup> J. R. Barber, Thermoelastic instabilities in the sliding of conforming solids, Proc. Roy. Soc. A. 312, (1969) 381-394.
- <sup>2</sup> TH. A. Dow and R. A. Burton, Thermoelastic instability of sliding contact in the absence of wear, Wear, 19 (1972) 315-328.
- <sup>3</sup> A. E. Anderson, R. A. Knapp, Hot spotting in automotive friction system, Wear, 135 (1990) 319-337.
- <sup>4</sup> H. Kasem, Thermal levels and subsurface damage induced by the occurrence of hot spots during high-energy braking, Wear, 270 (2011) 355-364.
- <sup>5</sup> Ralph A. Burton, Thermal deformation in frictionally heated contact, Wear, 59 (1980) 1-20.
- <sup>6</sup> P. Zagrodzki, Numerical analysis of temperature fields and thermal stresses in the friction discs of a multidisc wet clutch, Wear, 101 (1985) 255-271.
- <sup>7</sup> P. Zagrodzki, Analysis of thermomechanical phenomena in multidisc clutches and brakes, Wear, 140 (1990) 291-308.
- <sup>8</sup> P. Zagrodzki, Nonlinear transient behavior of a sliding system with frictionally excited thermoelastic instability, Journal of Tribology, Vol. 123 (2001) 699-708.
- <sup>9</sup> P. Zagrodzki, Samuel A. Truncone, Generation of hot spots in a wet multidisc clutch during short-term engagement, Wear, 254 (2003) 474-491.
- <sup>10</sup> P. Zagrodzki, Thermoelastic instability in friction clutches and brakes – Transient modal analysis revealing mechanism of excitation of unstable modes, International Journal of Solids and Structures, 46 (2009) 2463-2476.
- <sup>11</sup> S. Panier, P. Dufrenoy, J. F. Brunel and D. Weichert, Progressive waviness distortion: A new approach of hot spotting in disc brakes, Journal of Thermal Stresses, 28 (2005) 47-62.
- <sup>12</sup> Tien-Chen Jen, Daniel James Nemecek, Thermal analysis of a wet-disk clutch subjected to a constant energy engagement, International Journal of Heat and Mass Transfer, 51, 1757-1769, 2008
- <sup>13</sup> ABAQUS Theory manual 6.11